

Heat-capacity measurements on granular aluminum

R. L. Filler,* P. Lindenfeld, and T. Worthington†

Serim Physics Laboratory, Rutgers University, New Brunswick, New Jersey 08903

G. Deutscher

Department of Physics and Astronomy, Tel-Aviv University, Ramat-Aviv, Israel

(Received 14 September 1979)

We have measured the heat capacity of a series of films of aluminum in Al_2O_3 , with normal-state resistivities ρ_N from $2 \times 10^{-5} \Omega \text{ cm}$ to $4 \times 10^{-2} \Omega \text{ cm}$. The lattice heat capacity is greater than for the separate bulk constituents, but there is no evidence for a change in the electronic specific heat capacity. The specimens become superconducting with a heat-capacity transition which is BCS-like for low ρ_N and diminishes as ρ_N becomes greater than $10^{-3} \Omega \text{ cm}$, until it is no longer observable for the highest ρ_N . We conclude that as ρ_N increases the grains become decoupled. The size of the grains is such that thermodynamic fluctuations prevent the existence of bulk superconducting properties when they are isolated.

I. INTRODUCTION

Granular aluminum consists of metallic aluminum grains embedded in a matrix of aluminum oxide. Its normal and superconducting properties can be varied over a wide range by changing the proportions of its constituents, and have been the subject of considerable investigation and speculation. Depending on the amount of oxide between the grains, the electrical properties can be metallic, semiconducting, or insulating. Unless the amount of oxide is too large the material is superconducting, with transition temperatures which can be much larger than that of bulk aluminum.^{1,2}

In this paper we describe measurements of the heat capacity of a series of specimens whose normal-state resistivities range from 2×10^{-5} to $4 \times 10^{-2} \Omega \text{ cm}$. The increase in resistivity is the result of the presence of an increasing amount of oxide between the grains. For low resistivities the specimens behave like metals with a small electronic mean free path, and exhibit a discontinuity in the heat capacity at the superconducting transition in accord with the BCS theory. For higher resistivities the discontinuity diminishes until it is no longer observable. We interpret these results as showing that the grains become progressively decoupled until they are effectively isolated. The size of the grains (about 30 \AA) is such that thermodynamic fluctuations then prevent the continued existence of bulk superconducting properties.³

The measurements also lead to interesting results for the normal state. The lattice heat capacity is much larger than that of either metallic aluminum or crystalline aluminum oxide. It is likely that this is in part the consequence of the amorphous nature of the oxide, and in part the result of size and surface effects.

II. SPECIMENS

Pure aluminum was evaporated from an electron-beam source in the presence of a small amount of oxygen onto water-cooled glass substrates. A rate controller was used to keep the deposition rate at about $20 \text{ \AA}/\text{sec}$. In each evaporation a bridge-shaped specimen for electrical measurements was made at the same time as a specimen on specially thin glass for the heat-capacity measurements.

Our method of specimen preparation was similar to that described in Ref. 2. Our results show a comparable variation of the electrical transition temperature with the normal-state resistivity. We therefore assume that the other characteristics of the specimens were also similar in the two cases. Specifically we expect the grain size to be as determined in Ref. 2 by transmission electron microscopy, i.e., constant at about 30 \AA for values of resistivity greater than $10^{-4} \Omega \text{ cm}$.

The configuration of a heat-capacity specimen is shown on Fig. 1. The dimensions of the substrate are approximately 2 cm by 1 cm by $70 \mu\text{m}$, and the thickness of the evaporated film is about $10 \mu\text{m}$. A

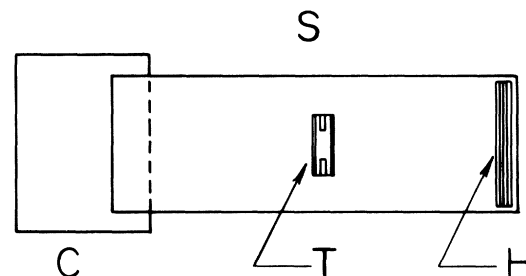


FIG. 1. Specimen configuration; H: heater, T: thermometer, C: copper tab, S: substrate.

copper tab is attached to the substrate at one end. At the other end a Constantan-film strain gauge is attached as a heater, and in the middle a thermometer made by sanding down an Allen-Bradley $\frac{1}{8}$ -watt resistor to a thickness less than that of the substrate.

Contact to the heater is made with two No. 42 Constantan leads, each about 1 cm long. The length of these leads is critical for the success of the experiment, since it affects the amount of heat developed in the leads as well as the amount of heat conducted through them. We assume that half of the heat developed in the leads flows toward the specimen and choose the length so that this amount of heat is approximately equal to the heat conducted away from the specimen during a heat pulse. Copper leads are used the rest of the way.

Constantan leads are also used to make contact to the thermometer. Three wires are used so that measurements can be made with a three-lead AC wheatstone bridge which allows cancellation of the lead resistance. All the wires to the heater and thermometer are attached with silver paint.

III. MEASUREMENTS

The heat capacity was determined by a pulse method which we have described earlier.⁴ A pulse of measured amplitude and duration is applied to the heater, and the response of the thermometer (ΔT) is recorded as a function of time (t). A signal averager is used to store and average about 20 pulses, and its output is then analyzed by a PDP-8 computer.

The computer fits an exponential to the decay of the pulse, starting at a time $2t_{\max}$, where t_{\max} is the time at which the temperature reaches its maximum. It then calculates the quantities⁵ $f_n = \int_0^{\infty} \Delta T t^n dt$ for $n=0, 1$, and 2 . From them it computes the diffusivity $D = \frac{11}{6} x^2 f_0 / f_1$ and the heat capacity for the portion of the specimen between heater and thermometer $C = \frac{6}{11} Q f_1 / f_0^2$, as well as the ratio $R = f_0 f_2 / f_1^2$ whose theoretical value is constant at 1.79. Q is the energy developed in the heater, and x is the distance between heater and thermometer.

The beginning of the pulse should have the same shape as a pulse on a specimen for which the distance from thermometer to bath is infinitely long,⁶ i.e., $\Delta T = Qx \exp(-x^2/4Dt) / C(\pi Dt)^{1/2}$. The computer calculates this function from the values of D and C which it has determined. Immediately after each measurement the curve so constructed from $t=0$ to t_{\max} is displayed on a 10-in. oscilloscope together with the averaged experimental curve of ΔT against t and the exponential fit to the decay portion of the curve.

Figure 2 shows a typical example. The values of C and D are kept and used only if visual inspection shows the fits to the beginning and to the decay of

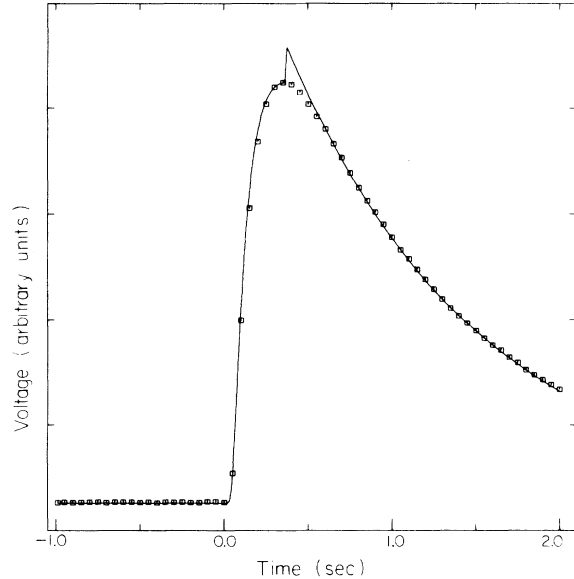


FIG. 2. Example of a temperature pulse. The points are the experimental data from the signal averager. (Every fifth point is shown.) The line from the maximum in the curve is an exponential fit to the data. The line up to the maximum is a fit using the equation described in the text. (Base-line temperature 2 K, $\Delta T_{\max} = 15$ mK.)

the pulse to be satisfactory, and if the ratio R is within about a percent of its theoretical value.

The size of the temperature excursion ΔT of the specimen thermometer was kept below 15 mK and near the transition usually considerably lower. The heat capacity of the substrate and addenda was measured in a subsequent run after carefully washing off the specimen *in situ* with cotton wool dipped in NaOH.

IV. NORMAL STATE

A. Results

The heat capacity in the normal state was assumed to follow the relation $C = \gamma T + AT^3$. The coefficients γ and A were determined from graphs of C/T against T^2 . Examples of graphs for several specimens are shown on Fig. 3. The values of the coefficients, and the other characteristic parameters of the specimens are shown on Table I.

A graph of γ as a function of the room-temperature resistivity ρ_N is shown on Fig. 4, and a graph of A against γ is shown on Fig. 5. On each of these graphs the point for pure aluminum is plotted as a square, and the point for our most impure specimen (specimen K , $\rho_N = 40 \times 10^{-3} \Omega \text{ cm}$) is plotted as a triangle. Specimen K is particularly interesting, but

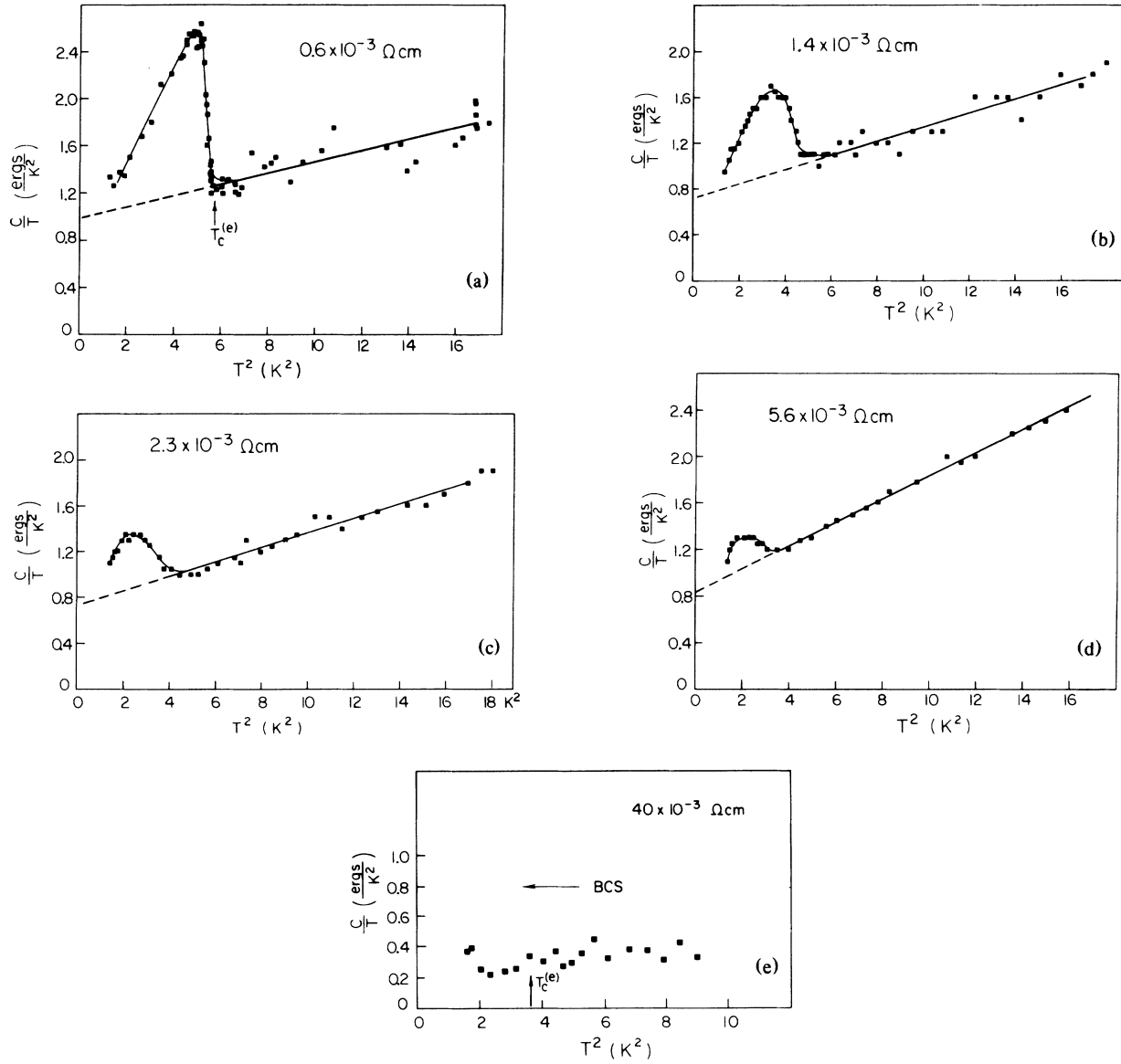
FIG. 3. C/T against T^2 for several specimens.

TABLE I. Characteristics of the specimens.

	Pure Al	A	B	C	D	E	F	G	H	J	K
ρ_N ($10^{-3} \Omega \text{ cm}$)	0.0028	0.013	0.02	0.3	0.6	1.4	2.3	2.7	2.8	5.6	40
$T_c^{(e)}$ (K)	1.2	1.8	2.0	2.0	2.35	2.36	2.30	2.1	2.23	2.06	1.90
t (μm)		11	14	10	10	10	10	10	11	10	6
γ ($\mu\text{J}/\text{K}^2\text{g}$)	50	36	29	21	27	20	20	17	19	23	
A ($\mu\text{J}/\text{K}^4\text{g}$)	9.2	15	19	27	13	18	17	44	15	28	
Θ (K)	428	360	330	300	380	340	350	250	370	300	

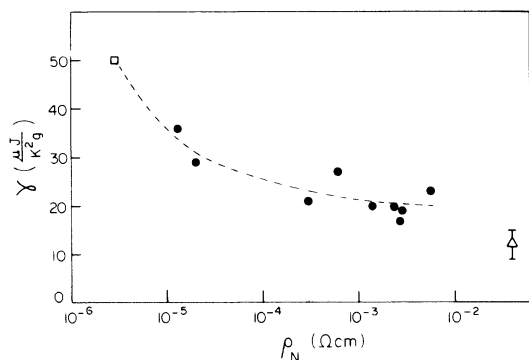


FIG. 4. The coefficient γ of the electronic specific heat capacity as a function of the room-temperature resistivity. The square represents the values for pure aluminum. The triangle is for specimen *K*.

unfortunately its measurement was subject to greater uncertainty than was the case for many of the other specimens. It was only about half as thick as the other specimens, and it was measured early in our experiment, before certain improvements leading to greater precision were made.

There are a number of reasons why the normal-state results are not as precise as the results for the superconducting state. They depend on measurements above the transition temperature, where the thermometer sensitivity is lower. The fraction of the heat capacity contributed by the substrate is larger in this region. Finally, the primary focus of our experiment was on the superconducting state, and fewer points were measured above T_c .

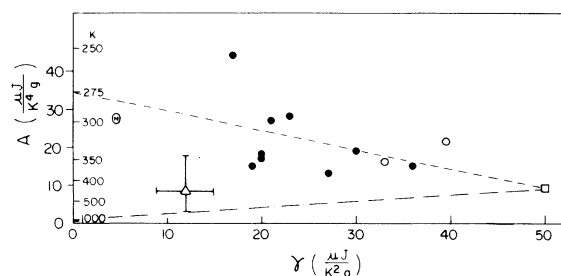


FIG. 5. The coefficient A of the lattice specific heat capacity as a function of the coefficient γ of the electronic specific heat capacity. The square is for pure aluminum and the triangle for specimen *K*. The lower line would be appropriate if the metal and the oxide components had the same lattice specific heat capacities as in the separate bulk crystalline materials. The upper line would be appropriate for a metallic component with the same specific heat capacity as in the bulk, and an oxide component with a Debye temperature of 275 K.

B. Discussion

The values of γ are consistent with the supposition that the specific heat capacity of the aluminum grains is the same as for pure bulk aluminum, so that the value of γ measured for the whole specimen is proportional to the fraction of metal which it contains. This assumption was also made by Greene, King, Zubeck, and Hauser⁷ for their measurements of the heat capacity of two granular aluminum specimens, and confirmed by them with independent determinations of the specimen composition.

For values of ρ_N between 10^{-4} and 10^{-2} Ω cm, γ is seen to vary very little, indicating that the resistivity varies rapidly for only a slight change in composition. We conclude that in this region the specimens are close to the percolation threshold of the system, and that for higher resistivities the grains can be expected to be largely separated from one another. The value of γ at the threshold corresponds to a volume fraction of metallic aluminum of about 40%, in good agreement with results on other granular aluminum systems.^{1,8} This supports the assumption that the electronic specific heat capacity of the grains does not vary substantially, at least up to the percolation threshold.

For the heat-capacity coefficients A and γ plotted on Fig. 5 we have used the values from Table I, i.e., the values which characterize the whole specimen. For a constant electronic specific heat capacity of the aluminum grains the horizontal axis is then proportional to the fraction of metal in each specimen. On the vertical axis we have also indicated the values of the Debye temperature which correspond to the various values of A .

The Debye temperature of bulk aluminum is 426 K, and for bulk crystalline Al_2O_3 it is 977 K. If the lattice specific heat capacities were the same in our specimens as for the two separate bulk crystalline constituents, the points of Fig. 5 would fall on the lower of the two straight lines. It may be seen that our measured points lie far above that line.

In Ref. 7 the values of both A and γ are ascribed to the metal grains only, on the assumption that the oxide behaves like crystalline Al_2O_3 and therefore contributes a negligibly small amount to the measured heat capacity. From the data in Ref. 7 we have calculated the coefficients corresponding to the whole specimens and plotted them as open circles on Fig. 5. It may be seen that they show an enhanced lattice heat capacity comparable to that of our specimens.

If we ignore for the moment the point for specimen *K* at the far left of the graph, the points are seen to cluster about the upper straight line. This line represents the linear superposition of the heat capacities of the metallic fraction with a Debye temperature equal to that of pure bulk aluminum, and an

oxide fraction with a Debye temperature of 275 K.

This procedure corresponds to an assumption opposite to that of Ref. 7, and ascribes the entire excess heat capacity to the oxide. It is possible that this is justified since the oxide is amorphous, so that its heat capacity should be larger than that of crystalline Al_2O_3 . The difference between the specific heat capacities of the crystalline and amorphous phases would, however, have to be unusually large.

Specimen *K* is seen to have a smaller lattice component than the other specimens. As mentioned earlier the uncertainty of the measurements for this specimen is greater than for the others, and any conclusions which depend on this specimen must therefore be very tentative. The lower value of its lattice heat capacity suggests that its state of aggregation may be somewhat more crystalline than that of the other specimens. This could be related to the fact that specimen *K* not only contains more oxide, but that the oxide is in larger pieces, while in the other specimens it is mostly in channels only a few angstroms wide. We are thus led to the suggestion that there may be different degrees of amorphism possible in this system. A similar conclusion was indicated for amorphous tin oxide on the basis of recent Mössbauer measurements.⁹

C. Comparison with results on other systems

Our measurements are not sufficiently extensive to allow us to distinguish between the contributions of the metal and the oxide to the lattice component of the heat capacity. The suggestion that the major part of the enhancement is to be ascribed to the oxide is supported by the measurements of Novotny and Meincke¹⁰ who found only small changes in the Debye temperature of lead and indium in porous glass.

Mössbauer measurements on granular tin also showed only small changes in the Debye temperature of the metal grains compared to that of bulk tin.¹¹ On the other hand, measurements on small vanadium particles showed substantial increases in both the electronic and the lattice components of the heat capacity.¹²

The same authors made measurements on palladium particles which showed large enhancements of the lattice heat capacity.¹³ In this case the electronic term was unchanged from the bulk, but the lattice term was no longer proportional to T^3 .

An attempt has been reported¹⁴ to determine the heat capacity of platinum particles cosputtered with SiO_2 . Small changes in the electronic heat capacity were reported, but were almost entirely obscured by changes and uncertainties in the silica matrix.

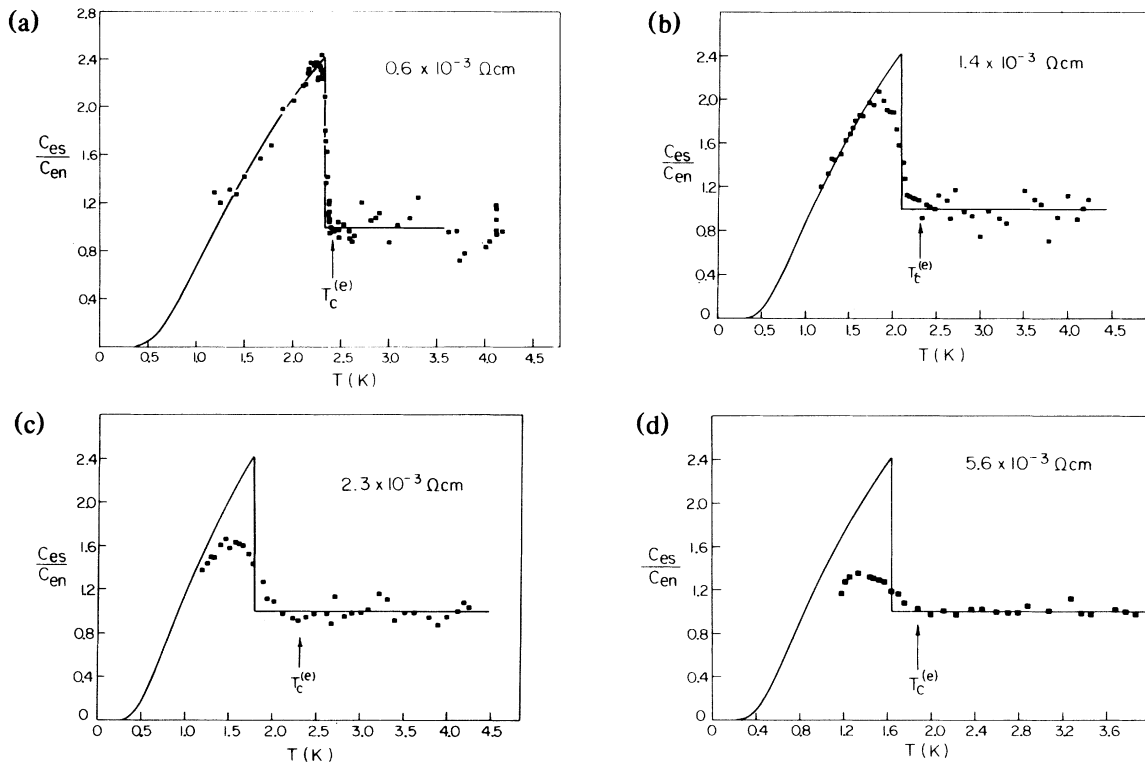


FIG. 6. The ratio of the electronic heat capacity in the superconducting state (C_{es}) to that in the normal state (C_{en}) for several specimens. The solid lines are the BCS curves for the transition temperature $T_c^{(c)}$ at which the measured value of C_{es}/C_{en} is halfway between its value in the normal state and the maximum. $T_c^{(e)}$ is the temperature at which the electrical resistance is half of its maximum value.

V. SUPERCONDUCTING STATE

A. Results

To determine the electronic heat capacity in the superconducting state, C_{es} , the lattice heat capacity, AT^3 , was subtracted from the measured heat capacity, leaving C_{en} , equal to γT , above the transition temperature, and C_{es} below. The ratio C_{es}/C_{en} for several specimens is shown on Fig. 6. Each of the curves also shows the theoretical (BCS) curve for a transition temperature $T_c^{(c)}$ equal to the temperature at which the measured C_{es}/C_{en} is halfway between its value of one in the normal state and its maximum value.

The curve for specimen *D*, with $\rho_N = 0.6 \times 10^{-3} \Omega \text{ cm}$, follows the BCS curve very closely. It has a sharp heat-capacity transition at a temperature $T_c^{(c)}$ which is essentially the same as the temperature $T_c^{(e)}$ at which the electrical transition takes place. This demonstrates the homogeneity of the specimen and gives us confidence in our method of specimen preparation and in our experimental procedure. The agreement between theory and experiment is much better than that for evaporated films previously measured in this laboratory⁴ and elsewhere.⁷

The curves for the specimens with greater values of ρ_N show a progressive decrease in the size of the heat-capacity transition, together with a lowering of $T_c^{(c)}$. A slower decrease, which becomes important only for values of ρ_N greater than $2.3 \times 10^{-3} \Omega \text{ cm}$, is observed for $T_c^{(e)}$. For the specimen with the highest value of ρ_N (specimen *K*, $\rho_N = 40 \times 10^{-3} \Omega \text{ cm}$) the heat-capacity transition is too small to be observed in our measurement, i.e., less than about 15% of the BCS value.

An electrical transition remains for specimen *K*, as shown in Fig. 7. $T_c^{(e)}$, the temperature at which the

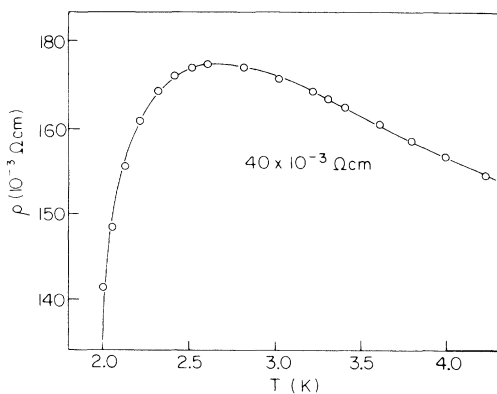


FIG. 7. The electrical resistivity as a function of temperature for specimen *K*.

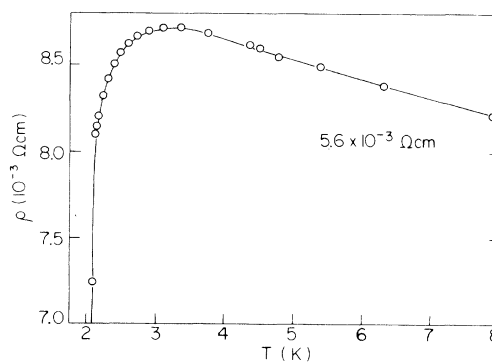


FIG. 8. The electrical resistivity as a function of temperature for specimen *J*.

resistance has fallen to half of its maximum value, is 1.90 K. The width, from 10 to 90%, is 0.54 K, consistent with the width expected from fluctuations. The electrical properties of this specimen have been discussed in a separate publication.¹⁵ The electrical transition of a somewhat purer specimen (specimen *J*, $\rho_N = 5.6 \times 10^{-3} \Omega \text{ cm}$) is shown on Fig. 8.

B. Discussion

The results shown on Fig. 6 demonstrate that the heat-capacity transition disappears as ρ_N goes approximately from 10^{-3} to $10^{-2} \Omega \text{ cm}$. It is known from work on other systems,⁸ and illustrated for our specimens on Fig. 4, that this change in resistivity corresponds to a very small change in composition.

We conclude that in this region the grains become sufficiently separated from each other to become decoupled, and that they are too small to have a measurable heat-capacity transition when they are isolated.

1. Isolated grains

The notion that there is a characteristic volume below which a specimen cannot have the properties of a bulk superconductor has been considered theoretically by a number of authors.¹⁶⁻¹⁸ The basic idea is that when the volume decreases the thermodynamic fluctuations increase and prevent a thermodynamic transition. A characteristic volume V_c is reached when the difference in free energy between the normal and superconducting states is equal to kT_c . The value of V_c is equal to $1/N(0)kT_c$, where $N(0)$ is the normal density of states at the Fermi level. For our system V_c is about $(50 \text{ \AA})^3$.

The heat capacity of an isolated grain has been calculated by Mühlischlegel, Scalapino, and Denton¹⁸

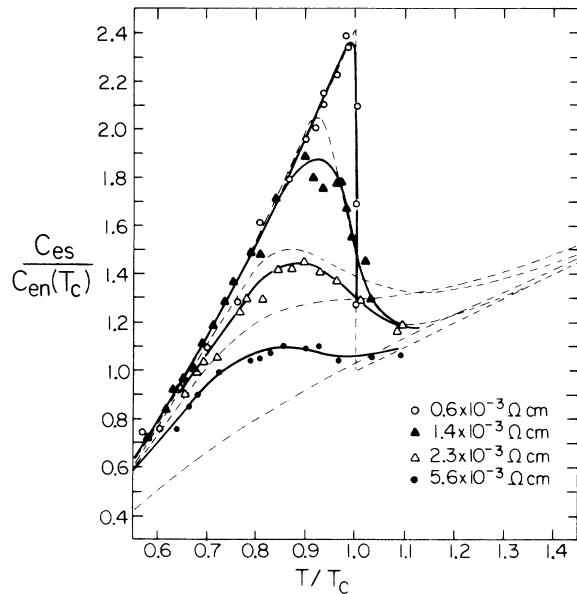


FIG. 9. The electronic specific heat capacity in the superconducting state divided by its value γT_c in the normal state at the transition temperature $T_c^{(c)}$. The solid lines are drawn through the experimental data. The dashed lines are the theoretical curves of Fig. 7 of Ref. 18 (MSD).

(MSD). Their results show that the heat-capacity transition diminishes and broadens as the grain size becomes smaller. The change in the heat capacity is about half of its value in the bulk when the volume of the grain is $10 V_c$, and about 3% of the bulk value when it is equal to V_c .

On Fig. 9 we have plotted the curves for our specimens together with those of MSD. It must be emphasized that the mechanism leading to the decrease in the heat-capacity transition is quite different in the two cases. For the MSD curves it is the size of an isolated grain that changes, while in our experiment it is the coupling between grains of roughly constant size.

The curves are seen to be similar, although we do not seem to observe the long tail above T_c which is present in the MSD curves. Furthermore the MSD calculations do not predict the observed decrease of $T_c^{(c)}$.

2. Coupling between grains

The coupling between grains has been considered in Ref. 19 using a model in which a simple cubic lattice of spherical grains is embedded in an insulating matrix, with Josephson coupling between the grains. A calculation of the thermodynamic fluctuations of the order parameter in this system shows that there is a strong-coupling regime and a weak-coupling regime, with a transition between them when ρ_N is approxi-

mately 10^{-3} to 10^{-2} Ω cm. In the weak-coupling regime the heat-capacity transition is that of the isolated grains. In our samples, which are in the small-grain limit, this transition should be so weak as to be unobservable. These predictions are in excellent agreement with our experiment.

It has been pointed out²⁰ that the model of Ref. 19 is incomplete in that it ignores the electrostatic energy E_c which results from electron transfer between grains. This energy tends to decouple the grains, counteracting the Josephson coupling energy E_J .

In Ref. 20 it is assumed that superconductivity will no longer be possible when E_c is greater than E_J . A more complete calculation has been made by McLean and Stephen,²¹ who show that in a three-dimensional system this criterion is too stringent by about one order of magnitude. A similar conclusion is reached on the basis of a model of de Gennes.^{3,22}

The value of E_c can, in principle, be calculated with the aid of the model of Abeles and his co-workers,^{1,23,24} which gives $E_c = (e^2/\epsilon_1 r)[s/(r+s)]$, where ϵ_1 is the dielectric constant of the insulator, r is the radius of the grain, and s is the distance between grains. The result, however, depends very sensitively on the value of s , especially for specimens near the percolation threshold, where s and E_c go to zero. We therefore prefer to estimate E_c by fitting the normal-state conductivity to their expression $\sigma = \sigma_0 \exp[-2(C/kT)^{1/2}]$. C is equal to $2\chi s E_c (1 + 1/2\chi s)$, where χ^{-1} is the decay length of the metallic wave function in the oxide. We tentatively approximate this relationship by using $2\chi s = 1$, so that C is about $2E_c$. This probably gives us an upper limit to the charging energy.

For specimen J ($\rho_N = 5.6 \times 10^{-3}$ Ω cm) between 4 and 8 K we then find $C = 5 \times 10^{-6}$ eV, or $E_c \approx 2.5 \times 10^{-6}$ eV.

We calculate E_J from the expression of Ambegaokar and Baratoff²⁵ and find, for $\rho_N = 5 \times 10^{-3}$ Ω cm and $d = 3 \times 10^{-7}$ cm, a value of about 6×10^{-5} eV. Electrostatic effects are therefore not important in this specimen. More generally we can conclude that electrostatic effects will not dominate as long as there is an observable heat-capacity transition, i.e., in the strong-coupling regime, where ρ_N is less than about 10^{-2} Ω cm.

For specimen K (40×10^{-3} Ω cm), in which only a resistive transition is observed, E_J is lower by a factor of about 7 because of the increase in resistivity, while E_c is larger. A fit to the variation of R with T gives $C = 1.5 \times 10^{-4}$ eV or E_c about 0.8×10^{-4} eV. We see that these energies just meet the criterion of McLean and Stephen²¹ so that charging effects can now be sufficiently large to prevent phase coherence of the grains. In specimens with higher resistivities no electrical transitions are observed.²

One can now attempt to account for the details of the experiment, such as the change in the shape of

the heat-capacity transition as it disappears, the progressive decrease of $T_c^{(c)}$ and $T_c^{(e)}$, and the persistence of a resistive transition when the heat-capacity transition is already unobservable. This requires that the effects of disorder be taken into account, since there is ample evidence that the metal-insulator transition in granular systems has to be described by percolation theory.¹

The problem is simplified by the likelihood that the distribution of grain sizes does not play an important role. This is so because our specimens are in the small-grain limit where individual grains do not have an observable heat-capacity transition, and because we have shown that the size-dependent electrostatic effects are not significant in the region of interest.

It is therefore sufficient to consider the distribution of coupling strengths. A percolation model has been developed in which grains with E_j greater than kT are considered as coupled, and grains with E_j less than kT as uncoupled.²⁶ The calculations based on this model reproduce the features of our experiment in all their detail.

C. Comparison with previous work

1. Isolated grains

There are only a few previous experiments which are directly related to our measurements. First there are two specific-heat experiments^{10,12} which have been referred to earlier. In both experiments only a small number of specimens were investigated, and the information on the superconducting transition depended on the subtraction of a large and perhaps uncertain lattice heat capacity.

In Ref. 10 three lead specimens (60, 37, and 22 Å) were measured showing a progressive broadening of the transition and lowering of the transition temperature with decreasing particle size. On the other hand, their single indium specimen (22 Å) had a sharp transition and an increased T_c .

Reference 12 describes work on two vanadium specimens, with average particle sizes of 65 and 38 Å. Again the transitions were broadened, but T_c went up with decreasing size.

In their measurements on palladium¹³ the same authors showed that the lattice heat capacity had a complicated temperature dependence. It is not known to what extent this affects the subtraction of the lattice term in other experiments, but all heat-capacity measurements on small particles which assume a T^3 dependence will have to be regarded with some suspicion until more is known about the temperature dependence of this term.

In our measurements, as well as in the measurements of Ref. 7 on the same system, there is no evidence for a departure from a T^3 dependence for the lattice term.

The broadening of the transitions in the lead and vanadium specimens is in qualitative agreement with our results. We cannot make a quantitative comparison since no attempt was made in Refs. 10 and 12 to compare their data to the BCS curves or to the curves expected for isolated grains.

The tunneling results of Zeller and Giaever^{27,28} on tin particles are considerably more extensive and detailed. The grains had average radii from 1700 to 18 Å. There was some evidence for superconductivity in all specimens. At the same time the structure in the tunneling characteristic which results from the presence of an energy gap became smaller and broader as the particle size decreased, until for an average radius of 30 Å there was no longer any evidence for an energy gap. These results are entirely consistent with our results and our interpretation.

2. Coupled grains

For the case of coupled grains there is also a tunneling experiment, namely that of Abeles and Hanak,⁸ which can be seen, in retrospect, to corroborate many of our results. At the time of its publication it could not, however, be regarded as decisive because of difficulties with its interpretation. It was not clear to what extent the tunneling measurements probed the bulk of the specimen rather than only the surface, and it was also not obvious to what extent the individual grains were being probed, and to what extent the results depended on the coupling between the grains.

The measurements were made on aluminum grains in SiO₂, with grain sizes like those of our specimens, i.e., about 30 Å at the highest oxide concentration of 40% by volume and a resistivity of 10^{-2} Ω cm. Near this critical concentration the resistivity increases rapidly and the energy gap goes precipitously to zero.

Although its authors considered the ambiguities of the interpretation to be too great to draw definite conclusions we can now review the situation with much greater confidence. A comparison with Fig. 1 of Ref. 8 shows that the critical values of the concentration and the resistivity, as well as the variation of T_c with ρ_N , are essentially the same as for our specimens.

Just as in our experiment, the rapid variation of ρ_N with concentration at the critical concentration shows that the grains are there becoming electrically decoupled from each other. The disappearance of superconductivity at this concentration shows that the isolated grains are then not capable of sustaining superconductivity. In all respects this behavior is the same as that which we observe.

A similar disappearance of superconducting behavior has also been observed in the magnetic susceptibility by Gershenson and McLean.²⁹ At low

resistivities their specimens behave like ordinary impure superconductors with penetration depths proportional to the square root of ρ_N . Above a value for ρ_N of about $8 \times 10^{-3} \Omega \text{ cm}$ the penetration depth increases much more rapidly with ρ_N , and evidence of bulk superconductivity disappears.

An experiment in which the coupling between grains is measured directly is that of Abraham, Deutscher, Rosenbaum, and Wolf.³⁰ In their experiment the critical current density of Al-Al₂O₃ films is determined for a series of films with different values of ρ_N . As ρ_N increases above $10^{-3} \Omega \text{ cm}$ the critical current density is seen to drop rapidly until superconductivity is no longer observed for ρ_N greater than about $10^{-2} \Omega \text{ cm}$.

Previous heat-capacity measurements on granular aluminum include the work of Greene, King, Zubeck, and Hauser,⁷ which we have already referred to. An experiment of Goldman, Solinsky, and Magee³¹ showed a complicated structure at the transition in specimens with relatively low values of ρ_N . In several runs with the requisite resolution and precision on similar specimens we saw no evidence of this structure.

VI. CONCLUSIONS

The literature on heat-capacity measurements on small metallic particles in the normal state is too chaotic and contradictory to allow any general conclusions. We content ourselves, for now, to note that in our measurements changes in the electronic specific heat are too small to be detected, and that there are large enhancements of the lattice heat capacity compared to that of either of the bulk constituents. We expect the enhancement to be, at least in part, the result of the amorphism of the oxide. We cannot tell whether it is also partly a consequence of size or surface effects of the aluminum grains.

The description of the transition to superconductivity is, by contrast, clear cut and unambiguous. In specimens with sufficiently low ρ_N the transition fol-

lows the BCS curve precisely.

As a corollary crucial for all other conclusions we note that this result demonstrates that the specimens behave for most purposes like macroscopically homogeneous, well-characterized materials with effective electronic mean free paths related to ρ_N .

As ρ_N increases the aluminum grains become decoupled and bulk superconductivity, as described by the heat-capacity transition, disappears. The disappearance is in excellent, detailed agreement with calculations which show it to be the result of thermodynamic fluctuations of the superconducting order parameter in the grains during the change from a strong-coupling to a weak-coupling regime.

In specimens with somewhat higher resistivities, for which no heat-capacity transition is observed, there can still be a resistive transition, apparently because of remaining percolation paths. The eventual disappearance of all superconductivity at resistivities greater than about $10^{-1} \Omega \text{ cm}$ is presumably the result of electrostatic effects.

The fact that no heat-capacity transition remains when the coupling is destroyed demonstrates that the grains are then no longer able to remain superconducting, at least in the BCS sense. Taken together with the results of Zeller and Giaever²⁷ this result leaves no doubt that thermodynamic fluctuations prevent the continued existence of superconductivity when the volume of the grains falls below the critical value V_c .

ACKNOWLEDGMENTS

We would like to acknowledge conversations with B. Abeles, P. G. de Gennes, M. Gershenson, Y. Imry, and W. L. McLean, as well as with the coauthors of Ref. 26. The research was supported by the National Science Foundation under Grant No. DMR 76-22962, by the Rutgers University Research Council, and by the U.S.-Israel Bi-national Science Foundation. Helium gas was supplied by the Office of Naval Research.

*Present address: U.S. Army Electronics, Technology, and Devices Laboratory, Fort Monmouth, N.J. 07703.

† Present address: IBM Thomas J. Watson Laboratory, Yorktown Heights, N.Y. 10598.

¹For a general review of this and other granular systems see B. Abeles, *Applied Solid State Science* (Academic, New York, 1976), Vol. 6, p. 1.

²G. Deutscher, H. Fenichel, M. Gershenson, E. Grünbaum, and Z. Ovadyahu, *J. Low Temp. Phys.* **10**, 231 (1973).

³A brief account of the superconducting properties has been published previously: T. Worthington, P. Lindenfeld, and G. Deutscher, *Phys. Rev. Lett.* **41**, 316 (1978).

⁴R. L. Filler, P. Lindenfeld, and G. Deutscher, *Rev. Sci. Instrum.* **46**, 439 (1975).

⁵M. Gershenson and S. Alterovitz, *Appl. Phys.* **5**, 329 (1975).

⁶B. Bertman, D. C. Heberlein, D. J. Sandiford, L. Shen, and R. R. Wagner, *Cryogenics* **10**, 326 (1970). A factor of 2 is missing in the numerator of Eq. (1) of this reference. Note also that their C is the specific heat per unit volume while ours is the heat capacity of a length x of the specimen.

⁷R. L. Greene, C. N. King, R. B. Zubeck, and J. J. Hauser, *Phys. Rev. B* **6**, 3297 (1972).

- ⁸B. Abeles and J. J. Hanak, *Phys. Lett. A* **34**, 165 (1971).
- ⁹G. S. Collins, T. Kachnowski, N. Benczer-Koller, and M. Pasternak, *Phys. Rev. B* **19**, 1369 (1979).
- ¹⁰V. Novotny and P. P. M. Meincke, *Phys. Rev. B* **8**, 4186 (1973).
- ¹¹S. Akselrod, M. Pasternak, and S. Bukshpan, *J. Low Temp. Phys.* **17**, 375 (1974); *Phys. Rev. B* **11**, 1040 (1975).
- ¹²G. H. Comsa, D. Heitkamp, and H. S. Råde, *Solid State Commun.* **20**, 877 (1976).
- ¹³G. H. Comsa, D. Heitkamp, and H. S. Råde, *Solid State Commun.* **24**, 547 (1977). This paper contains references to work on aluminum and silver particles which also show increased lattice heat capacities.
- ¹⁴G. R. Stewart, *Phys. Rev. B* **15**, 1143 (1977).
- ¹⁵W. L. McLean, P. Lindenfeld, and T. Worthington, in *Electrical Transport and Optical Properties of Inhomogeneous Media*, edited by J. C. Garland and D. B. Tanner, AIP Conf. Proc. No. 40 (AIP, New York, 1978), p. 403.
- ¹⁶V. V. Schmidt, *Zh. Eksp. Teor. Fiz., Pis'ma* **3**, 141 (1966) [*JETP Lett.* **3**, 89 (1966)].
- ¹⁷G. Deutscher, *Phys. Lett. A* **35**, 28 (1971).
- ¹⁸B. Mühlischlegel, D. J. Scalapino, and R. Denton, *Phys. Rev. B* **6**, 1767 (1972).
- ¹⁹G. Deutscher, Y. Imry, and L. Gunther, *Phys. Rev. B* **10**, 4598 (1974).
- ²⁰B. Abeles, *Phys. Rev. B* **15**, 2828 (1977).
- ²¹W. L. McLean and M. J. Stephen, *Phys. Rev. B* **19**, 5925 (1979).
- ²²P. G. de Gennes (private communication).
- ²³P. Sheng, B. Abeles, and Y. Arie, *Phys. Rev. Lett.* **31**, 44 (1973).
- ²⁴B. Abeles, Ping Sheng, M. D. Coutts, and Y. Arie, *Adv. Phys.* **24**, 407 (1975).
- ²⁵V. Ambegaokar and A. Baratoff, *Phys. Rev. Lett.* **10**, 486 (1963).
- ²⁶G. Deutscher, O. Entin-Wohlman, S. Fishman, and Y. Shapira, *Phys. Rev. B* **21**, 5041 (1980) (following paper).
- ²⁷H. R. Zeller and I. Giaever, in *Superconductivity, Proceedings of the International Conference on the Science of Superconductivity*, edited by F. Chilton (North-Holland, Amsterdam, 1971), p. 173.
- ²⁸H. R. Zeller and I. Giaever, *Phys. Rev.* **181**, 789 (1969).
- ²⁹M. Gershenson and W. L. McLean (unpublished).
- ³⁰D. Abraham, G. Deutscher, R. Rosenbaum, and S. Wolf, *J. Low Temp. Phys.* **32**, 853 (1978).
- ³¹A. M. Goldman, J. C. Solinsky, and T. J. Magee, *J. Low Temp. Phys.* **20**, 339 (1975).